

Pedestal Signature Characterization in the FWedges  
of the D0 Silicon Multistrip Tracker

A senior Honors Project

Presented to

the Department of Physics, Astronomy, and Materials Science

and the Honors College

Southwest Missouri State University

In Partial Fulfillment

of the requirements for

Departmental Distinction in the Honors College

by

Justace Clutter

May 2004

PEDESTAL SIGNATURE CHARACTERIZATION IN THE FWEDGES  
OF THE D0 SILICON MULTISTRIP TRACKER

Department of Physics, Astronomy, and Materials Science

Southwest Missouri State University, May 2004

Justace Clutter

A B S T R A C T

The Silicon Multistrip Tracker sub-detector in the D0 particle detector at the Fermi National Accelerator Laboratory is plagued with noise and interference patterns. This paper will bring to light two prominent interferences, anti-correlation and grassy noise. A root cause for either interference pattern was not found during an initial investigation. However, details of each interference are listed along with the techniques to find them. A promising technique to quantify grassy noise is presented along with proof that the grassy noise present in the Micron FWedge sensors is bias voltage dependent.

Pedestal Signature Characterization in the FWedges  
of the D0 Silicon Multistrip Tracker

by

Justace Clutter

A senior Honors Project  
Submitted to the Honors College  
Southwest Missouri State University  
in Partial Fulfillment of the Requirements  
for Departmental Distinction in the Honors College

May 2004

Approved:

---

Project Director

---

Department Head

---

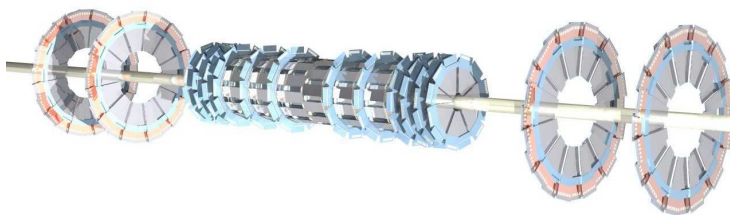
Dean of the Honors College

# Contents

<b>1 Silicon Multistrip Tracker Introduction</b>	<b>1</b>
1.1 Geometry . . . . .	1
1.2 SVXIIe . . . . .	3
1.3 High Voltage Supply . . . . .	4
1.4 Data Chain . . . . .	5
<b>2 FWedge Noise</b>	<b>6</b>
2.1 Desired Signature . . . . .	6
2.2 Anti-Correlation Signature . . . . .	8
2.3 Grassy Noise . . . . .	9
<b>3 Conclusions</b>	<b>14</b>

# 1 Silicon Multistrip Tracker Introduction

The D0 particle detector at the Fermi National Accelerator Laboratory is composed of several different layers. Each layer of this detector focuses on generating a specific subset of the physics data required to increase the overall knowledge of proton/anti-proton, or  $p\bar{p}$ , collisions. The Silicon Multistrip Tracker, or SMT, is the first stage of the detector that post collision particles interact with, as long as the beam pipe is neglected. In general, the SMT is a collection of over 800,000 small strip PIN diode detectors in a known geometrical configuration. When a charged particle traverses a region of a PIN diode, an assortment of electron/positron pairs are generated. The number of generated pairs is commensurate with the energy of the incident particle. For the purpose of the D0 detector, the amount of energy deposited in the SMT is desired to be very low. The motivation for this desire is to allow for the calorimeter to measure the energy of the particle accurately. During an “event”, a mass of particles is generated and passed through the SMT. The current generated by this traversal is first collected in an integrating amplifier, and then converted to a digital signal by the SVXIIe analog to digital conversion chip. This per strip data is collected and collated into clusters. These clusters are then passed through a centroid style algorithm that determines both the center and magnitude of the interaction. This information allows the track fitting algorithm to determine the particle paths, resulting in the acquisition of the physics parameters. The remainder of this section will focus on the physical aspects of the D0 SMT.

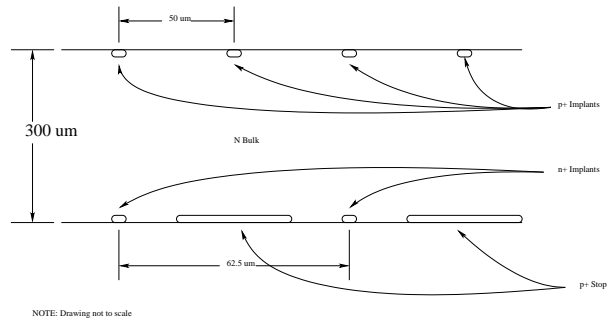


## 1.1 Geometry

The D0 SMT is composed of three different geometries; Barrels, FDisks, and HDisks. There are four HDisks, two at each end; twelve FDisks and six Barrels intermixed in the center. Each one of

these top level assemblies are then further broken down into small components. The HDisks and FDisk are reduced to a collection of twenty-four HWedges and twelve FWedges respectively. The barrels are broken down into a number of differently sized rectangular detectors based on their radial distance from the beam-line.

In order to reduce the scope of this project, the FDisk was the only data source for the study. As a by-product of this, the remainder of the paper will only discuss topics directly related to the FDisk and their associated FWedges. When designing the FWedges, it was decided to use a double sided detector. The benefit of going with a double sided detector is the ability to calculate a radial component of the interaction even though the detector is oriented perpendicular to the beam-line. The two sides of the FWedge will be denoted as  $P$  and  $N$ , corresponding to the doping used for the channels.



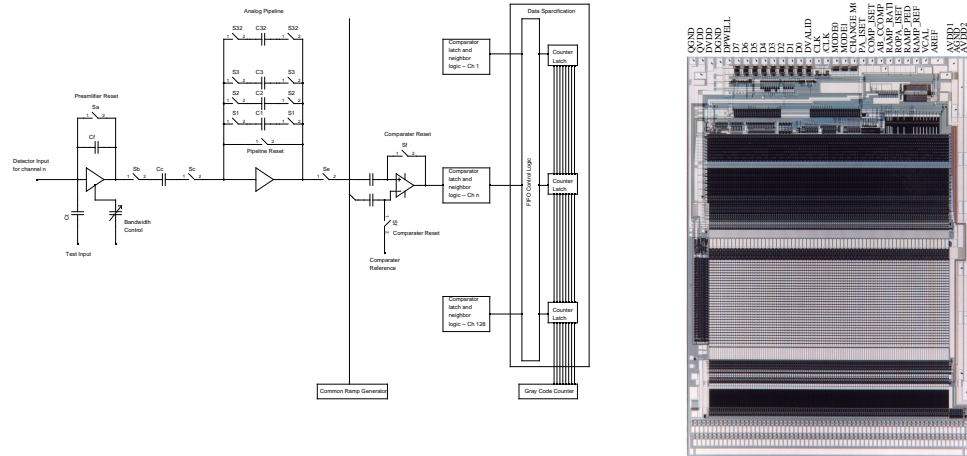
The  $P$  side of the wedge has 1024 channels with a pitch of 50 microns, while the  $N$  side has only 768 with a pitch of 62.5 microns. The strip density reduction in the  $N$  side of the wedge is driven by the  $p+$  implants inbetween the  $n+$  implants. These “ $p+$  stops” were needed to channel the electric field correctly around the  $n+$  implants. The strips, here on known as channels, are set at an angle of  $15^\circ$ . By taking these angles on both sides into account, there is a total stereo angle of  $30^\circ$  between the strips of the two wedges. This stereo angle allows for a radial position measurement from the interaction point in the center of the beam mentioned earlier.

For the D0 detector, two different manufacturers produced the silicon sensors used in the SMT; Micron and Eurysis. It should be noted that there are subtle differences in the two sensors from the different manufacturers. The Micron detectors have a different guard ring structure than the

Eurysis along with a different  $p+$  stop implementation. The Eurysis engineers added a  $p$ -spray to the side with the  $p+$  stops. This  $p$ -spray, which is a low level  $p+$  implantation, was applied to the entire surface. The  $p$ -spray, guard ring structure, and overall general quality assurance in the manufacturing process place the Eurysis based wedges in first place according to the noise performance.

## 1.2 SVXIIe

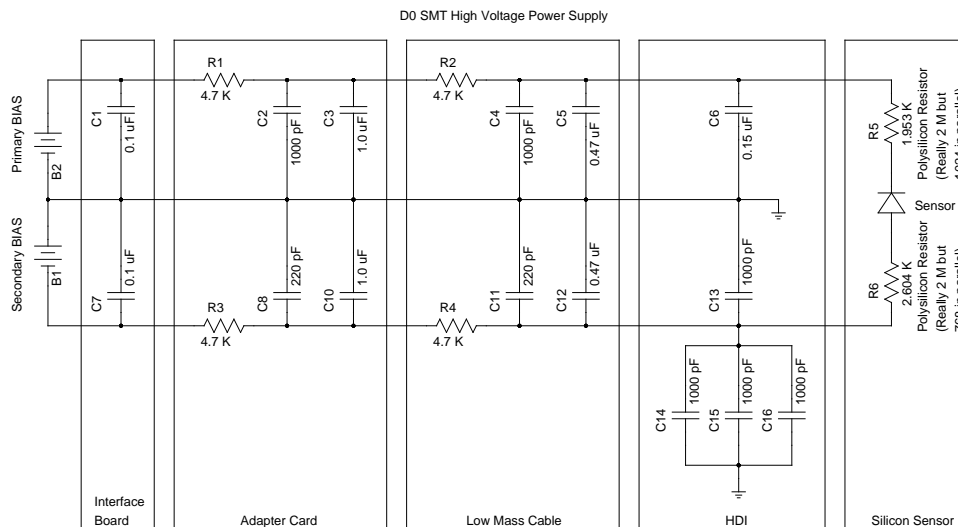
The SVXIIe is a third generation chip custom engendered for the requirements of the CDF and D0 detectors at Fermilab. It was designed to maintain the same noise characteristics of it's predecessor, the SVXI, and provide electronics to enable interaction times of 132 ns. [2] The die, based on a 1.2 micron process, contains 128 individual channels with a small array of common sub-circuits. Each channel combines an integrating amplifier, a capacitor bank for an analog storage pipeline, a comparator, and finally an RS latch. The common circuits in the SVXIIe are a ramp generator and grey code counter. The output of the PIN diode is integrated on the incoming amplifier during the acquire mode of the chip. This signal is then placed in the storage pipeline until it is time to be converted in digitize mode. When the digitize mode begins, the grey code counter is reset and is incremented at each clock cycle. This continues until the voltage entering the comparator matches the voltage present on the storage capacitor. Since the comparator output changes to the opposite rail on the inversion of the input signals, the comparator output can be used to drive the latch. As soon as the comparator output changes, the latch is actuated and the current grey count is stored in the latch. When readout mode is initiated, the data in the latch is placed on the 8 bit bus that is carried out on the high density interconnect. The dataflow past this point is discussed in the section entitled "Data Chain" later in this document. Below is a SVXIIe channel schematic along with a selectively annotated photo-micrograph of the SVXIIe chip.



### 1.3 High Voltage Supply

In order to create the required electric field in the PIN diode to collect the generated electron/positron pairs, an electric field must be established. This electric field is generated by reverse biasing the PIN junction. The SMT high voltage, or HV, biasing system is sourced through HV pods in the second floor movable counting house. There are several different ways to bias a silicon sensor for this purpose. The method chosen for the double sided silicon is called split biasing, and requires two HV pods. One of the pods supplies a positive potential and is applied to the  $N$  side of the detector. This is often called the primary bias. The other pod supplies a negative potential and is connected to the  $P$  side of the detector, and following the naming convention is referred to as the secondary bias. These two HV lines are carried to the sensor over a single high mass/low mass cable chain for the FWedges. Since the potentials are carried to the FWedge on a single cable chain, the HV destined for the  $P$  side of the wedge is wrapped around the wedge to the far side from the  $N$  side on a flex cable.

Once the HV has been delivered to the FWedge, the lines are connected to a BIAS ring that encapsulates the wedge sensor. Each channel is then connected to this BIAS ring through a 2 M $\Omega$  polysilicon resistor. The resistance of this component has been known to fluctuate to high values and due to quantity requirements, resistances of up to 10 M $\Omega$  were allowed to pass quality assurance. A circuit representing the D0 SMT HV system is shown below.



It should be noted that the circuit given above is for a single wedge.  
 If studying the FWedges in the detector one needs to realize  
 that there could be up to four of these circuits in parallel  
 sharing the supply voltages

## 1.4 Data Chain

After the data is generated at the chip level, it is passed through several different layers of hardware devices. The need for these different levels is two fold, signal transportation and data rate. The distance between the detector and the movable counting house is far enough to require the need to transport the data through a fiber line. After the date has arrived at the movable counting house it must be stored in several different buffers. It is through these buffers that a data rate high enough for D0 is attainable.

The pedestal data leaves the chip on an eight bit bus printed on a flex circuit called the high density interconnect, or HDI. This HDI is then connected to a similar flex circuit called the low mass cable. The low mass cable is unique since it combines the flex circuit technology with a long circuit. Two of these low mass cables come together on an adapter card that places the signals on a single eighty conductor cable, often referred to as the high mass cable. This eighty conductor cable is connected to one of the four slots on an interface board which is the convergence point for the chip low voltage power supply, the sensor high voltage supply, and the bi-directional data bus. After the data passes through the interface board it is handed off to a sequencer where it is encoded on a single fiber line that goes to a VTM. The VTM converts the fiber signals to electrical signals that

the VRB can understand. The VRB is a large buffer that holds the data before it is passed to the single board computer, or SBC. The SBC then uses the in-place network to transfer the data to one of the many computers in the farm node network where it is analyzed. After the data has been analyzed by the farm, it is passed to the Feynman Computing Center for storage and eventual later retrieval for further analysis.

## 2 FWedge Noise

### 2.1 Desired Signature

As any detector, the SMT FDisks suffer from the regular noise patterns that are inherent to any electronic measurement device. In reference to silicon devices there are three main types of noise. The total power from a particular noise type is generally the following. [1]

$$P_{\text{type}} = \int_{f_1}^{f_2} p(f)df \quad (1)$$

In this equation the  $p(f)$  term represents the power density as a function of the frequency. Noise can be characterized by the interaction of the power density and the frequency. This normally generates two main categories,  $\frac{1}{f}$  noise and white noise. The white noise is characterized by its flat spectral response and contains two main noise forms, thermal and shot noise. The most prominent noise source is thermal and is referred to as either Johnson or Nyquist noise. The charge carriers inherently have a certain amount of agitation based on their thermal temperature. This agitation results in a non-uniform instantaneous current flow, which is observed as noise. The power density function,  $p_T(f)$ , for thermal noise is reproduced below. [1]

$$p_T(f) = k_B T \Delta_f \quad (2)$$

In the above equation  $\Delta_f$  represents the bandwidth of the measuring device,  $k_B$  is the Boltzmann constant, and  $T$  is the temperature in Kelvin. It is easy to see that since the power density is not

related to the frequency, the noise is directly related to the temperature linearly. The temperature control in silicon detectors is vital for this reason. The second noise type in the white regime is called shot noise. This noise is related to the quantum nature of the fundamental charge magnitude. It is related to fluctuations in a steady average current flow. This differs from the thermal noise which does not depend on the average current. The formalism for the shot noise is the follows. [1]

$$I = \sqrt{2qI_D\Delta_f} \quad (3)$$

The result of this equation is the root mean square of the amperes related to the shot noise. The equation is dependent on the square root of the electron charge, the forward junction current, and the bandwidth of the measuring device. It is known that the magnitude of the shot noise is reduced by several orders of magnitude in a reverse biased configuration. In most cases, the shot noise may be neglected. In the case of the SMT where all the PIN diodes are reverse biased, the shot noise may certainly be neglected.

The final noise type,  $\frac{1}{f}$ , is dominant at low frequencies. It is sometimes known as flicker noise and has no known stable cause. flicker noise is represented in all active devices and is related to the DC biasing current. In situations related to silicon, the  $\frac{1}{f}$  noise is based on crystal structure deformation and contamination levels. Flicker noise is known to follow a relationship close to the following. [1]

$$I = \sqrt{m \frac{I^a}{f^b} \Delta_f} \quad (4)$$

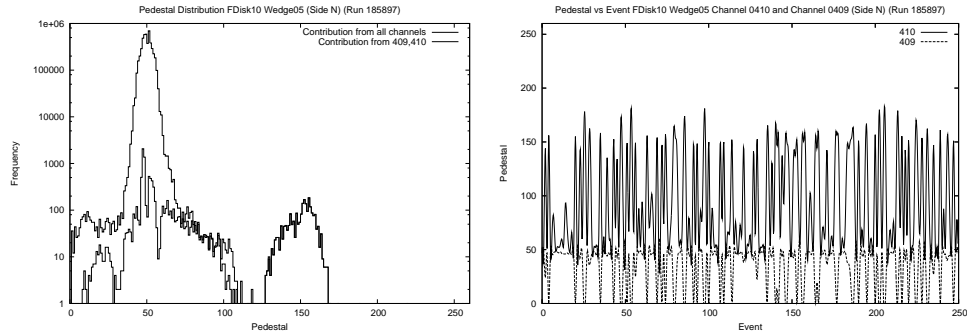
The  $m$  term is a specific value related to the component being observed while  $a$  ranges from .5 to 2 and  $b$  ranges from .8 to 1.2.

With these different noise types summed together the standard deviation of a normal channel in the SMT averages a value close to two or three. It is assumed that any standard deviation exceeding this value is due to another source. The noise sources listed above are intrinsic to the circuit itself, therefore, these other effects must be related to an external source, albeit a manufacturing defect

or interference from another subcircuit in the D0 detector. The retrieved data of a good FWedge, without a beam present, should look like a regular Gaussian distribution centered on the mean pedestal value. In a situation where a particle beam is present the pedestal distribution takes on a Landau form. Based on early analysis of the pedestal data from the SMT, two signatures were the focus of the remainder of the study, anti-correlation and grassy noise. The following two sections discuss these two signatures and bring to light the properties of each.

## 2.2 Anti-Correlation Signature

Some of the FWedges exhibit a pedestal distribution such that there are several preferred values with smaller distributions around them. After studying into the problem more in depth, it was found that there are normally two channels that account for the strange distribution. One channel will take on several different values above the average pedestal while the second channel in the pair will take on values below the average pedestal. This is represented in the following plots from FWedge05 from FDisk10.



The pedestal distribution plot accentuates the contribution from the responsible channel pair, channels 409 and 410. By plotting these two channels as a function of event, pseudo function of time, a strong anti-correlation can be found. This signature has been found numerous times in different FWedges and several realizations can be made from the observations.

1. Effect always comes in channel pairs
2. One channel always takes multiple high values while the other channel always takes low values
3. Statistical correlations between channels is very close to -1

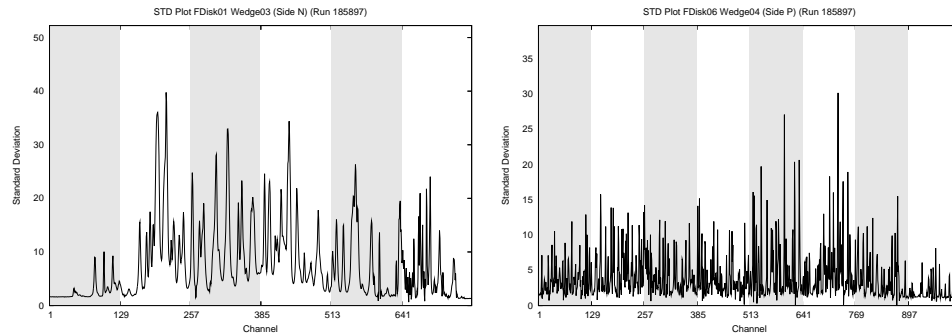
4. Effect is present both with and without high voltage biasing on the sensor

By joining these realizations together, it is possible to generate a few deductions. It is obvious that the problem is not sensor related since the effect is not dependent on sensor biasing. Since the effect is observed in neighboring channel pairs, the obvious point to concentrate on is the interaction point in the data sparcification region. After focusing on this section of the chip, it becomes a possibility that the problem is based on the latch interaction with the output bus. If one channel populates the bus with its gray count, and the next channel is told to populate there is a possibility for failure. The failure mode is generated in the following way. With the bus populated with the first channel's data, channel two actuates its latch to fill the bus with its data. If the second channel latch does not operate correctly, the bus will have mixed data on it, some from the first channel and some from the second channel.

After observing the data, it became clear that the probability for this failure mode is very low. The description above would only produce one channel that behaved improperly, when in fact there are two. A more acceptable failure mode would be a single channel read out on top of two channels. The single channel that would be read out would cross the 8 bit boundary. This would account for the multiple high values with a single distribution of low values between the paired channels. A problem for this mode is the returned gray coded values. The highest bit in the returned gray code values very seldom contain a 1. There are cases where the upper value goes above 128, in which case this value would be high, but that is very rare. More work on this problem is required, but, it is easy to state that the problem is digital and most certainly in the neighboring channel interaction point on the chip.

### **2.3 Grassy Noise**

The grassy noise signature is characterized by a specific pattern in the standard deviation versus channel plots for the FWedges. The pattern represents a collection of grass from a yard if viewed from the ground level.



The original theorized cause of the grassy noise was based on microdischarge effects. It was thought that discontinuities in the deposited layers would cause a high electric field, resulting in a microdischarge. It would be easy to state this if the discharge was present in just a few locations along the surface of the sensor. From looking at the data, much the same way that the anti-correlation signature was studied, the following can be stated regarding the grassy noise.

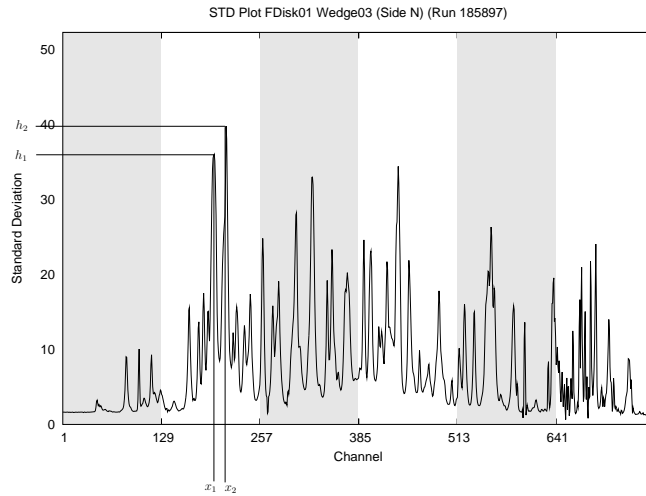
1. Dependent on high voltage bias value
2. Based on the standard deviation, possible “discharging” occurs at specific locations
3. Primarily present on the Micron based sensors (For differences between Micron and Eurysis see section 1.1)

In order to characterize the amplitude of the grassy noise as a function of a given variable, a good metric was required. In the beginning, grassy noise was searched for visually in the pedestal distributions for a given run. It was thought the noise would appear as a strong nominal value with a long tail to the right. The distribution was decidedly different than a Landau distribution that could be described with the above description. The primary difference is the falloff slope in both directions of the nominal value. In a Landau, the slope to the lower values is much higher than the slope to the higher values. In the no-beam pedestal distributions, the falloff slopes were symmetrical. A key aspect to the visual inspection was the log scaling in the histogram.

Due to the sheer number of FWedges, this process took an extended amount of time. A shift to using a more computational method was needed. In order to accomplish this shift, a processing technique based on the standard deviation plots was used. A third order equation was fit to the standard deviation versus channel data for each wedge and the resulting  $\chi^2$  value was returned. The

motivation for using this factor was based on the theory that the grassy noise would have a high residual amount after the fitted function subtraction where a smooth line would have a much lower value for the residual. The  $\chi^2$  parameter then became a direct indicator of grassy noise. One might question the validity of using a third order equation and ask why not use a second order equation. The simple answer is that the third order equation allows for the built-in fitting of the background noise in the channels of the wedge. As the strip length becomes shorter the noise is reduced and this is prominently observed in the standard deviation versus channel plots.

This metric became questionable after the realization that if the majority of the FWedge has the noise and it is all at about the same level then the  $\chi^2$  value would return a low value. The  $\chi^2$  technique also did not take into account for peak density. In several instances, there are channels that have a high standard deviation not related to grassy noise. These channels are often spread out on the FWedge. Therefore a new metric that took into account local density and amplitude would increase the probability of producing usable results.

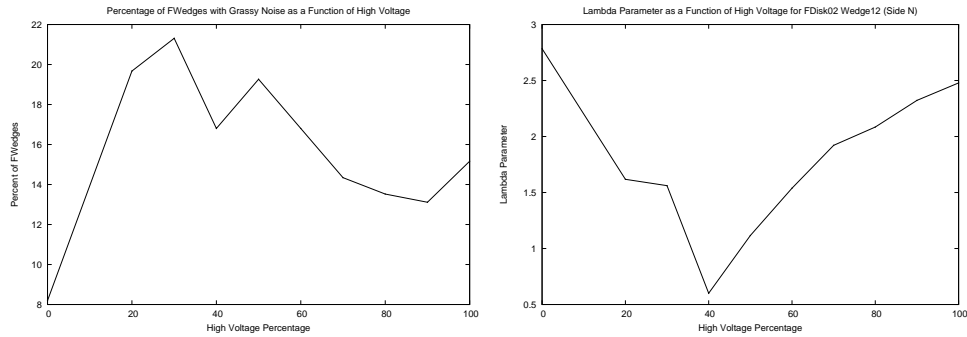


In the above plot, the new metric is applied to the first standard deviation plot presented in the beginning of this section. Since the metric should rise as the amplitude and also rise as the separation between the two peaks reduces, the following is used.

$$\lambda = \frac{h_1 + h_2}{2(x_2 - x_1)} \quad (5)$$

By calculating the average metric value,  $\bar{\lambda}$ , over an FWedge, a number representative of the grassy component can be found. A visual comparison with the results of the  $\lambda$  metric and the standard deviation plots exhibits a good result. It could be stronger by refining the peak finding algorithm. Currently the data smoothing filter used on the dataset is a single static flutter value.

During the spring beam shutdown of this year, several datasets were taken in read-all mode with varying high voltage bias settings. From this set of data, a determination of the high voltage dependence of the grassy noise can be attained.



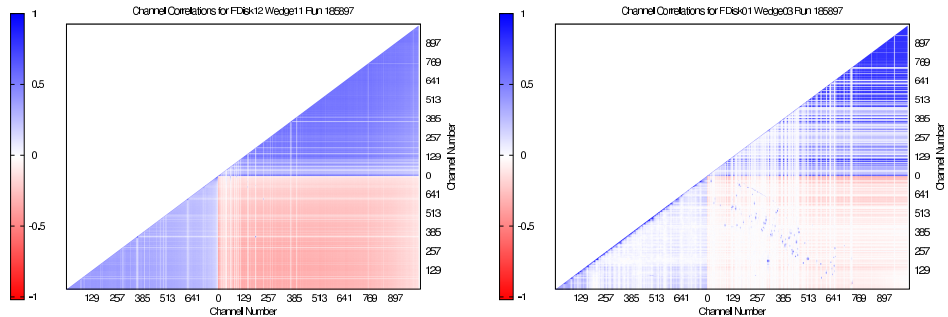
The plots are missing information on a high voltage setting of ten percent due to problems in reducing that dataset. Also of concern is that the percentage calculations assume that there are 288 working FWedges in the system. This, in general, is not true and that number should have been reduced by 20% based on normal operating numbers. The minimum at 40% high voltage is strange but real. The data points on either side of the 40% point are in-line with the reduction. From these plots it is easy to see a high voltage dependence on the grassy noise.

In an effort to derive more information on the grassy noise structure, correlation data was generated. Due to the computational volume in such measurements, the correlation matrix was calculated for a limited number of FWedges. The function to calculate the correlation is below.

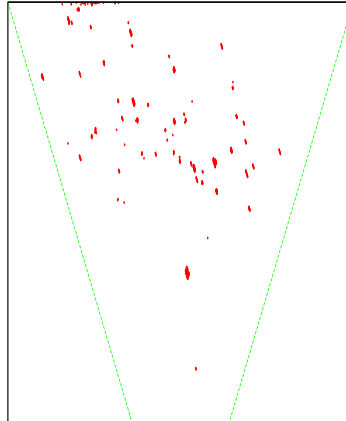
$$\text{corr}(c_i, c_j) = \sum_n \frac{(c_{i,n} - \bar{c}_i)(c_{j,n} - \bar{c}_j)}{\sigma_i \sigma_j} \quad (6)$$

Where  $c_i$  and  $c_j$  represent the pedestal values of channel  $i$  and channel  $j$  respectively and  $n$  is the number of events in the dataset. In addition with calculating the channels of a single wedge correlated with itself, the correlations with the opposing side of the wedge were also calculated. If

the basis for the grassy noise is in fact related to microdischarge events, a correlation between the two opposing sides would be present. Due to the stereo angle of the channels discussed in section one, the physical position on the FWedge can be determined from the correlation data. Below are two correlation matrixes, one for a grassy noise FWedge and one for a normal FWedge.



The axes in the correlation plots presented above pertain to the channel number on the FWedge. Looking at the  $x$  axis, the scale ranges from 0 to 768, then from 0 to 1024. The splitting is related to the number of channels on the  $N$  side and the  $P$  side of the wedge, the first section corresponding to the  $N$  side. The numbering scheme on the  $x$  axis is replicated on the  $y$  axis which allows for all the possible correlation combinations for a single wedge to be presented in a single plot. The plot can be broken down into three different regions; the lower left is the  $N$  side correlated to itself, the upper right is the  $P$  side correlated with itself, and the lower right rectangle represents the correlations from the  $N$  side to the  $P$  side. For these plots, the interesting region is the lower right rectangle. As can be seen, the plot on the left corresponds to a clean FWedge while the plot on the right corresponds to a grassy FWedge. By choosing a threshold of .5 the cross correlations in the grassy noise example can be mapped to specific regions on the FWedge.



Although the correlation data can not be used alone to look for defects in the sensor, it is possible to attain specific regions that warrant a more detailed analysis. In an effort to reduce the grassy noise signature, the existing data will have to be reanalyzed to look for a minimization of the noise as a function of high voltage. This data has already been produced; however, the peak finding algorithm needs to be redesigned to be more robust. A new dataset containing information on the high voltage dependence could be useful to verify the grassy noise minimization currently found at 40% based on the  $\lambda$  metric.

### 3 Conclusions

The FDisks in the D0 SMT sub-detector have been analyzed from a noise signature standpoint. This analysis has generated just as many questions as it has answered along with the realization that the cause of both signatures is still unknown. It is vital to the data from the D0 detector that the noisy channels found in these signatures be discarded. If the noisy channels are included in the cluster generation, the possibility for false tracks present itself. Future work on this project will focus on ensuring that noisy channels are in fact not being allowed to advance to the clustering algorithm.

## References

[1] Joshua Israelsohn. Noise 101. *Electronic*, January 2004.

<http://www.reed-electronics.com/ednmag/article/CA371088?pubdate=1%2F8%2F2004>.

[2] R.Yarema. *A Beginners Guide to the SVXIE*.